UDC 612.825.1+612.826

C. C. LEE[1] and K. IMAIZUMI[1]

FUNCTIONAL CONVERGENCE OF THALAMIC AND INTRINSIC PROJECTIONS TO CORTICAL LAYERS 4 AND 6

Received June 06, 2013.

Ascending sensory information is conveyed from the thalamus to layers 4 and 6 of the sensory cortical areas. Interestingly, receptive field properties of cortical layer-6 neurons differ from those in layer 4. Do such differences reflect distinct inheritance patterns from the thalamus, or are they derived instead from local cortical circuits? To distinguish between these possibilities, we utilized *in vitro* slice preparations containing the thalamo-cortical pathways of the auditory and somatosensory systems. Responses from neurons in layers 4 and 6 that resided in the same column were recorded using whole-cell patch clamp. Laser-scanning photostimulation via uncaging of glutamate in the thalamus and cortex was used to map the functional topography of thalamo-cortical and intracortical inputs to each layer. In addition, we assessed the functional divergence of thalamo-cortical inputs by optical imaging of flavoprotein autofluorescence. We found that the thalamo-cortical inputs to layers 4 and 6 originated from the same thalamic domain, but the intracortical projections to the same neurons differed dramatically. Our results suggest that the intracortical projections, rather than the thalamic inputs, to each layer contribute more to the differences in their receptive field properties.

Keywords: thalamus, cortex, auditory, somatosensory, intracortical circuits, photostimulation

INTRODUCTION

In the sensory forebrain, thalamo-cortical axons branch and synapse in layers 4 and 6 of their target cortical areas [1-4]. These branched projections enable ascending sensory information to be conveyed directly and in parallel to each cortical layer. Supporting such parallel streams, the short-term synaptic plasticity of thalamo-cortical inputs to both layers 4 and 6 are similar, exhibiting depressing postsynaptic responses to repetitive electrical stimulation [5-9] similar to those observed at other synapses in the sensory forebrain [10-12].

Interestingly, despite the direct nature of the thalamo-cortical inputs to these layers, receptive field properties in layer 6 are distinct from those in layer 4 [13-18]. For example, spectral and temporal modulation preferences differ between layers in the auditory cortex,, with layer-6 units responding to broader spectral and lower temporal modulations compared to those in layer 4 [14]. Tuning preferences likewise vary among layers in the visual [13, 16] and somatosensory [15, 17] cortices. This arrangement poses a dilemma, and it, therefore, remains an open question whether such differences in receptive field properties among layers reflect distinct inheritance patterns from the thalamus, or these differences are derived instead from local cortical circuits or another mechanism.

Indeed, all layers of the cortex receive convergent inputs from a wide constellation of intrinsic cortical sources, which comprise over half of the total number of convergent inputs from combined thalamic and cortical sources [19-21]. Intrinsic synapses outnumber those arising from thalamic sources. In the visual cortex, for example, thalamic synapses comprise only about 5% of the total innervation on layer-4 thalamorecipient neurons [22, 23]. Thus, the intricate and prolific connections from local cortical circuits are potentially poised to refine and modulate the information arriving through the ascending thalamo-cortical streams [12, 24-26].

Therefore, to explore the relative contributions of

[1] Department of Comparative Biomedical Sciences, LSU School of Veterinary Medicine, Baton Rouge, Louisiana, USA
Correspondence should be addressed to: C. C. Lee
(e-mail: cclee@lsu.edu)

thalamic and intracortical projections to layers 4 and 6, we utilized *in vitro* slice preparations containing the intact thalamo-cortical pathways of the auditory and somatosensory systems. Responses from neurons in layers 4 and 6 that resided in the same column were recorded using whole-cell patch clamp. Laser-scanning photostimulation via uncaging of glutamate in the thalamus and cortex was used to map the functional topography of thalamo-cortical and intracortical inputs. In addition, optical imaging of flavoprotein autofluorescence in the cortex in response to thalamic stimulation was used to assess the spatial and temporal pattern of activity in layers 4 and 6 following thalamic stimulation.

METHODS

Slice Preparation. Thalamo-cortical slices were prepared from BALB/c mice (age p11-p18). Animals were first deeply anesthetized by isofluorane, as assessed by cessation of withdrawal reflexes to strong toe-pinches. Following decapitation, the brains were quickly dissected and submerged in cool oxygenated artificial cerebrospinal fluid (ACSF; composition in mM: NaCl, 125, $NaHCO_3$, 25, KCl, 3, NaH_2PO_4, 1.25, $MgCl_2$, 1, $CaCl_2$, 2, and glucose, 25). Brains were then blocked to preserve the thalamo-cortical projections to either the primary auditory cortex (A1) [27] or primary somatosensory cortex (S1) [28]. The blocked brains were affixed to a stage with instant glue adhesive; then, 500-μm-thick sections were collected in cold oxygenated ACSF using a vibratome (World Precision Instruments, USA). Collected slices were transferred to a holding chamber for 1 h at 32°C in ACSF and then moved to a recording chamber perfused with ACSF at 32°C on a modified microscope stage (Siskiyou, Grants Pass, USA).

Recording, Photostimulation, and Optical Imaging. Neurons were visualized under DIC optics on an Olympus BX-51 upright microscope equipped with a U-DPMC intermediate magnification changer with 0.25× and 4× intermediate lenses (Olympus America, USA), rear-mounted with a Hitachi KP-M1AN camera (Hitachi, USA) and front-mounted with a Retiga-EX camera (QImaging, Canada). Whole-cell voltage clamp recordings were made using the Multiclamp 700B amplifier and pCLAMP software (Molecular Devices, USA) or Ephus software (Janelia Farms, USA). Recordings were performed in the voltage clamp mode using a potassium intracellular solution (in mM: K-gluconate, 135, NaCl, 7, HEPES, 10, Na_2ATP, 1–2, GTP, 0.3, $MgCl_2$, 2; pH 7.3 and 290 mOsm). Cytoarchitectural and anatomical markers determined laminar positions of the neurons, as we have previously demonstrated [9, 24, 25]. The lower border of layer 4 was apparent by the transition from small densely packed neurons to larger, more sparsely packed neurons in layer 5 [29, 30]. In the somatosensory slices, layer 4 was readily identifiable by the canonical barrel and septal regions [9, 28]. Similarly, the borders of layer 6 were determined by the white matter and transition to the large, sparsely packed neurons in layer 5 [9, 24, 25]. Depolarizing current injections were used to determine spiking characteristics of the recorded neurons. Regular-spiking (RS) neurons were classified as firing at slow adapting frequencies (<30 sec^{-1}) with small and slow afterhyperpolarizations (AHPs; 5–10 mV), while fast-spiking (FS) neurons were classified according to higher maximal firing rates (>30 sec^{-1}) and large and fast AHPs (10–15 mV). The acquired data were recorded and digitized using a Digidata 1440A acquisition board (Molecular Devices) or a National Instruments BNC 2090 terminal block (National Instruments, USA) and then stored in a computer for subsequent analysis.

Laser-scanning photostimulation (LSPS) with caged glutamate was used to map the thalamic and cortical regions eliciting EPSCs in the recorded layer-4 or -6 neurons of interest [9, 25, 31]. After patching, a recirculating ACSF bath containing nitroindolinyl(NI)-caged glutamate (0.37 mM; Sigma-RBI, USA) was switched in place of the regular ACSF bath. Direct responses to photostimulation were determined by using a solution containing caged glutamate in a low-Ca^{2+} (0.2 mM) / high-Mg^{2+} (6 mM) ACSF solution with TTX (1 μM), and synaptic responses were estimated by subtraction. Photolysis of the caged glutamate was done focally with a pulsed UV laser (DPSS Lasers, Inc., USA). Custom software (Ephus) written in MATLAB (MathWorks Inc., USA) was used to control the galvanometer mirror positioning of the laser beam for photostimulation and to analyze the data [32]. We used a 16×16 stimulation array with 80 μm spacing between adjacent rows and columns. Previous controls demonstrated that laser uncaging of glutamate elicits action potentials (APs) within 40-50 μm with respect to the soma [25, 33]. The mean EPSCs elicited from three map repetitions were averaged, and the interpolated plots were superimposed on photomicrographs corresponding to

the stimulation sites. Thalamic and laminar boundaries were determined from cytoarchitectural landmarks in the DIC images [9, 33]. The ventrobasal (VB) nucleus was discerned as a dark crescent-shaped structure with fibers traversing it laterally [9, 28]. The medial geniculate body (MGB) was visualized as an almond-shaped structure that was lighter in brightness than the laminated structure of the lateral geniculate nucleus (LGN) rostrally and the darker appearance of the ventrobasal complex medially [9, 27, 33]. The thalamic region projecting to a given recorded layer-6 neuron was measured from the thalamic photostimulation sites that elicited EPSCs and normalized to the region eliciting EPSCs of the recorded layer-4 neuron in the same column. The averaged mean EPSCs were totaled from each stimulation site in both the thalamus and cortex for a given neuron to determine the normalized contribution (%) from each thalamic and intracortical source. Statistical comparisons of distributions of numerical data were performed using StatPlus (AnalystSoft, USA).

Metabolic activity in response to thalamic stimulation was measured with the front-mounted Retiga-EX camera (QImaging) by capturing green light (~510–540 nm) generated by mitochondrial flavoproteins in the presence of blue light (~450–490 nm) [34]. Optical images were captured over 12-sec runs using Streampix 5.13 (Norpix Inc., Canada) following electrical stimulation in the thalamic regions projecting to the cortical areas being imaged. Electrical stimulation was performed using a concentric bipolar electrode (WPI, USA) to deliver a repetitive stimulation train of 100 sec^{-1} lasting for 500 msec and controlled by a Master-9 pulse generator (A.M.P.I., Israel) at stimulation intensities of 50-200 μA adjusted using an A365R stimulus isolator (World Precision Instruments, USA). The image exposure time ranged from 80 to 150 msec. Images were taken at a 4× magnification and processed using custom software written to run on Matlab [34, 35]. Spatial and temporal signal profiles were analyzed using ImageJ (NIH, USA). Defined regions of interest (ROIs) were used to measure changes in the pixel intensity within or across cortical layers. For temporal analyses, ROIs in the center of maximal activation in layers 4 or 6 in the same column were chosen, and the change in intensity across image stacks (time) was plotted for each layer.

***In vitro* tract-tracing.** Following physiological recordings, selected slices were transferred for post-fixation to a 4% paraformaldehyde solution (Electron Microscopy Sciences, USA) in 10 mM phosphate-buffered saline (pH 7.3). DiI crystals (Life Technologies, USA) were carefully placed with a needle into the thalamic nuclei (VB or MGB) of thalamocortical slices under a dissecting microscope (AmScope, USA). Slices were covered with aluminum foil and incubated in the dark at room temperature for 2-3 months. Following adequate lipophilic diffusion of DiI into thalamo-cortical fibers, slices were mounted between two pieces of coverglass with Vectashield hard set mounting medium (Vector Labs, USA). DiI-labeled fibers were then visualized using a Leica TCS SP2 confocal laser-scanning microscope (Leica Microsystems, USA) housed in the microscopy center at the LSU School of Veterinary Medicine. Acquired images were analyzed using ImageJ (NIH).

RESULTS

In order to assess the connectivity of the thalamocortical slice preparations, DiI crystals were placed into the respective thalamic nuclei in the auditory and somatosensory slices (Figs. 1, 2). In the auditory preparations (Fig. 1), thalamo-cortical fibers

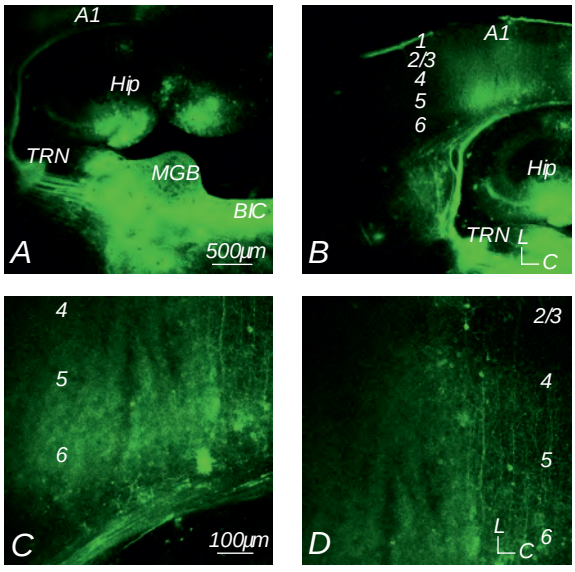

Fig. 1. Thalamo-cortical projections in an auditory slice preparation. A) Placement of DiI crystals in the medial geniculate body (MGB). Labeled fibers traverse toward the thalamic reticular nucleus (TRN) continuing onward towards the primary auditory cortex (A1). B) Thalamo-cortical fiber terminations in the A1. C) Labeled axonal fibers and retrogradely labeled cells in layer 6. D) Labeled fibers extending to layer 4.

Рис. 1. Таламо-кортикальні проекції в слайс-препараті слухової кори.

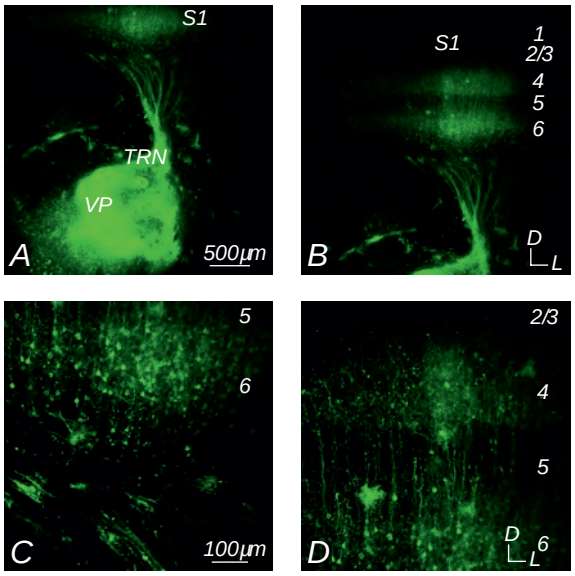

F i g. 2. DiI tracing of projections in the somatosensory thalamo-cortical slice. A) DiI crystal placement in the ventroposterior nucleus (VP) and fibers traversing to the primary somatosensory cortex (S1). B) Fiber terminations in the primary somatosensory cortex. C) Axonal fibers and retrogradely labeled cells in layer 6. D) Labeled fibers extending to layer 4.

Р и с. 2. Виявлення проекцій у слайсі таламуса і соматосенсорної кори.

originated from the medial geniculate body (MGB) and traversed rostrally towards the thalamic reticular nucleus (TRN) (Fig. 1A). There they ramified profusely before continuing laterally towards the cerebral cortex (Fig. 1B). As these fibers approached the primary auditory cortex (A1), they rerouted caudally before entering the deep cortical layers (Fig. 1B, C). Upon entering the deep layers, the fibers branched in layer 6 before continuing towards the upper cortical layers (Fig. 1D). This pattern was similar, but somewhat more continuous, to that described earlier [27]. In the somatosensory slice preparations (Fig. 2), thalamo-cortical fibers traversed laterally from the ventrobasal complex to the TRN before curving dorsally towards the primary somatosensory cortex (S1) (Fig. 2A, B), where they formed a distinct band in layers 4 and 6 of the S1 (Fig. 2C, D). In both auditory and somatosensory slices, retrogradely labeled cell somata were observed in layer 6 (Fig 1C, 2C), indicative of the robust feedback projections from the cortex to the thalamus [36-38].

To further characterize the thalamo-cortical projections in these slice preparations, we utilized optical imaging of flavoprotein autofluorescence (FA)

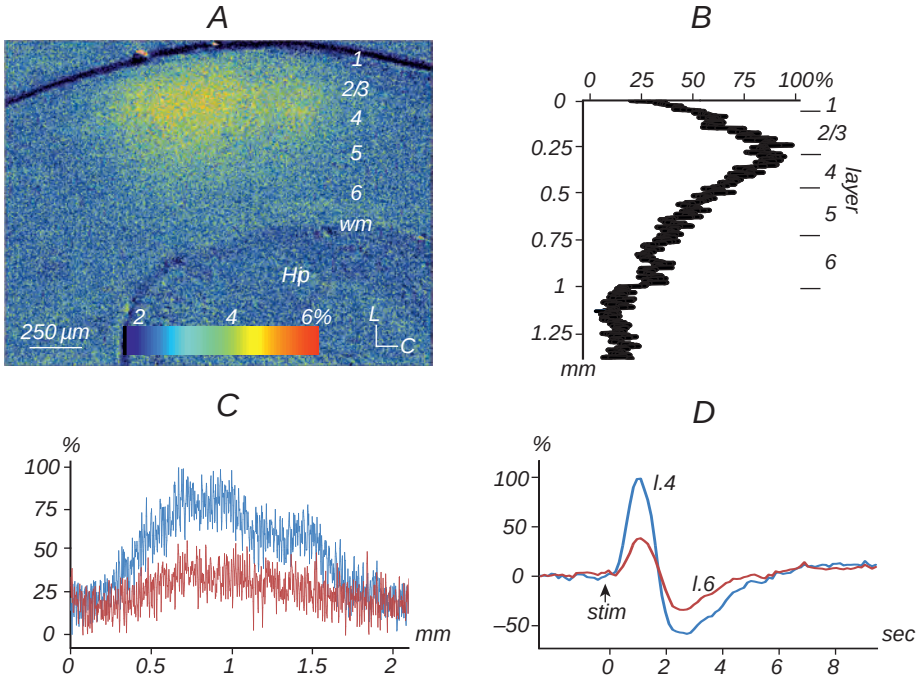

F i g. 3. Areal and laminar activation pattern of flavoprotein autofluorescence (FA) in the auditory cortex (zone A1) following electrical stimulation of the MGB. A) FA image of the A1 at the time of maximal autofluorescence following thalamic stimulation. B) Laminar FA profile in the A1 at the time of maximal autofluorescence. C) Areal profile of FA responses across layers 4 and 6. D) Time course of a cortical FA response in layers 4 and 6 of the A1.

Р и с. 3. Зонний і ламінарний патерни аутофлуоресценції флавопротеїнів (FA) в слуховій корі (зона *A1*) після електричної стимуляції медіального колінчастого тіла.

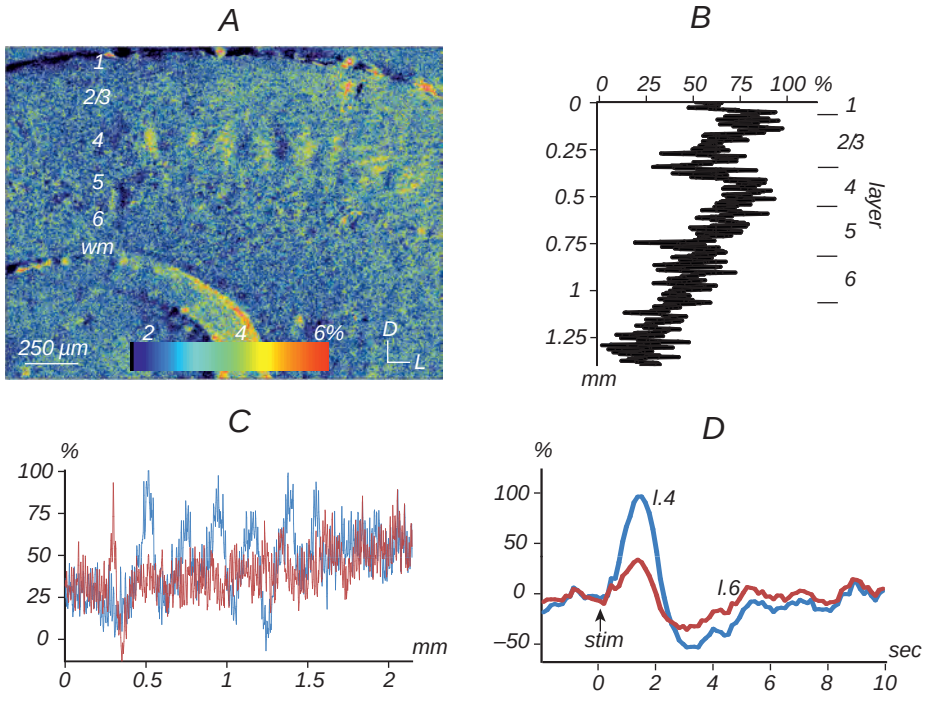

F i g. 4. Areal and laminar activation pattern of flavoprotein autofluorescence (FA) in the somatosensory cortex (area S1) following electrical stimulation of the VPm. A) FA image of the S1 at the time of maximal autofluorescence following thalamic stimulation. B) Autofluorescence responses across layers at the time of maximal FA response. C) Areal profile of FA responses across layers 4 and 6 in the S1. D) Time course of the cortical FA response in layers 4 and 6 of the S1.

Р и с. 4. Зонний і ламінарний патерни аутофлуоресценції флавопротеїнів у соматосенсорній корі (зона *S1*) після електричної стимуляції заднього вентрально-медіального ядра таламуса (*VPm*).

in the cortex following electrical stimulation of the thalamus (Figs. 3, 4). We found robust FA activation in the primary auditory and somatosensory cortices, which peaked approximately 1 sec following thalamic stimulation and was observed in both layers 4 and 6 (Figs. 3D, 4D). At the time of maximal activation, robust autofluorescence was especially visible in layers 3 and 4 of the auditory cortex (n = 3), with weaker activation in lower layers, including layer 6 (Fig. 3A, B). Despite the difference in the intensity among layers 4 and 6 (Fig. 3B), the areal extent of the activation was similar for both layers 4 and 6, originating at similar rostral-caudal extremes and cresting at the same rostral-caudal location (Fig. 3A, C). In the primary somatosensory cortex (n = 3), autofluorescence was most prevalent in the barrel regions of layer 4 and decreased in the upper and lower cortical layers (Fig. 4A, B). The barrel architecture resulted in a periodic areal pattern of activation across the S1 in layer 4, which was not evident in layer 6 (Fig. 4A, C).

We further sought to compare the functional convergence of inputs to pairs of neurons in layers 4 and 6 in the auditory and somatosensory systems using whole-cell patch clamp recordings of cortical neurons in response to laser-scanning photostimulation (LSPS) via uncaging of glutamate (Figs. 5, 6) [9, 24, 25, 33]. In each slice preparation, we recorded from regular-spiking (RS) neurons in layers 4 and 6 (A1, n = 6 pairs; S1, n = 10 pairs) residing along a presumptive cortical column, as determined by cytoarchitectural and anatomical boundaries. We then mapped the topography of LSPS-evoked EPSCs in the thalamic and cortical areas projecting to the recorded neuron. In both the auditory (Fig. 5) and somatosensory (Fig. 6) slices, we found that the areal extent and location of the thalamus that elicited EPSCs in layer-4 (Figs. 5A, 6A) and layer-6 (Figs. 5B, 6B) neurons were similar to each other (Figs. 5E, 6E) (layer 6 to 4 ratio: A1, 99 ± 43%; S1, 108 ± 31%; combined, 103 ± 35%). The mean evoked currents to layer 6 were, however, weaker than

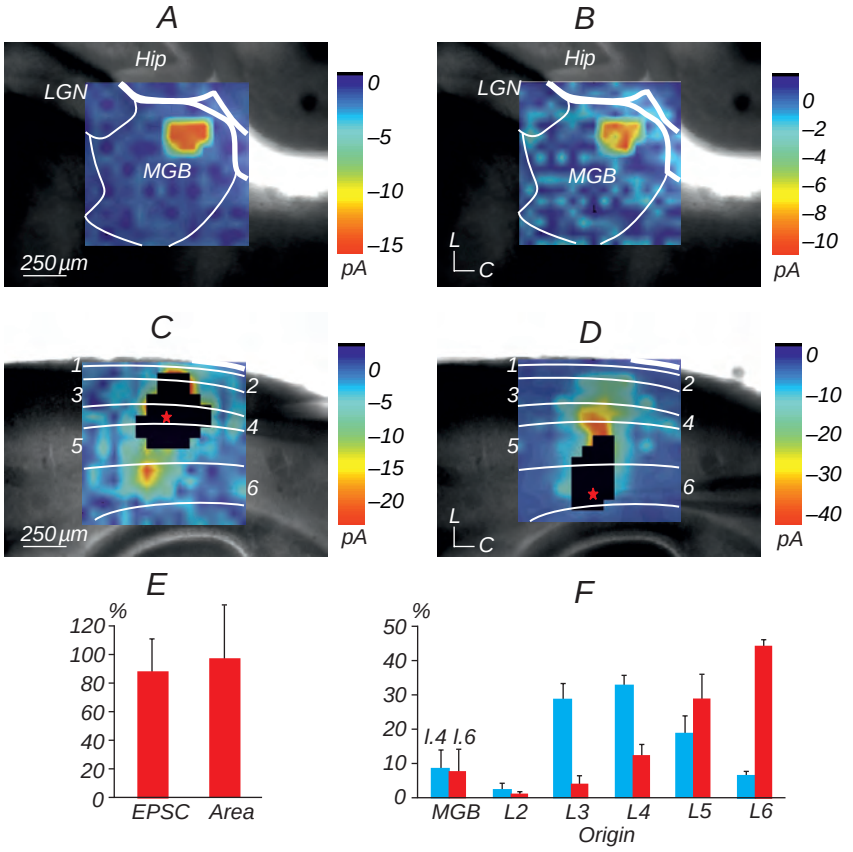

F i g. 5. Auditory thalamo-cortical and intracortical inputs to layers 4 and 6 of the A1. A-D) Average LSPS plots of mean EPSCs recorded in a layer-4 neuron (A,C) or a layer-6 neuron (B,D) in response to photostimulation of the medial geniculate body (MGB; A-B) or auditory cortex (A1; C-D). Filled regions in *C* and *D* illustrate direct response areas of the recorded neurons. E) Mean thalamic area and mean total evoked current in layer 6 normalized to that of layer-4 neurons recorded in the same column. F) Mean percentage of total current elicited from the MGB and layers 2-6 in either the layer-4 neuron (blue) or layer-6 neuron (red).

Р и с. 5. Слухові таламо-кортикальні та внутрішньокортикальні входи до шарів 4 і 6 зони *A1*.

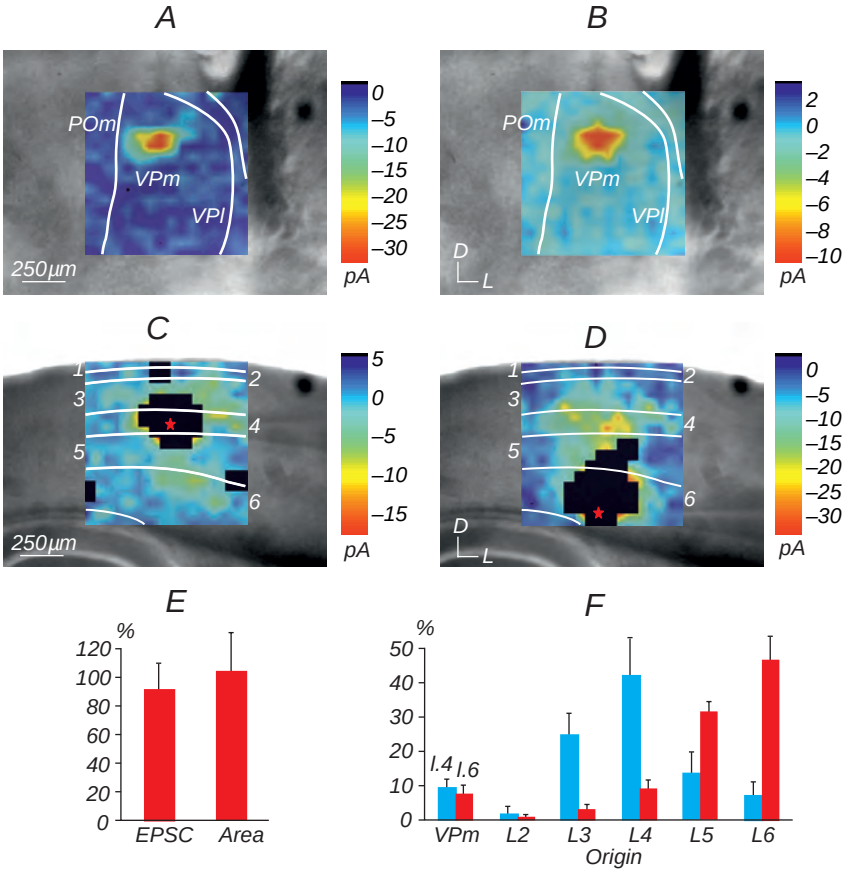

F i g. 6. Somatosensory thalamo-cortical and intracortical inputs to layers 4 and 6 of the S1. A-D) Photostimulation of the ventral posterior medial nucleus (VPm; A-B) or primary somatosensory barrel cortex (area SI; C-D). Plots illustrate averaged mean EPSCs . Filled regions in *C* and *D* illustrate direct response areas of the recorded neurons (E) Mean area evoking EPSCs in the thalamus and the mean total evoked current from the VPm in layer 6 normalized to that of layer 4. F) Mean percentage of total current elicited from the VPm and layers 2-6 in either the layer-4 neuron (blue) or the layer-6 neuron (red).

Р и с. 6. Соматосенсорні таламокортикальні та внутрішньокортикальні входи до шарів 4 і 6 зони *S1*.

Table 1. Normalized intensity, %, of mean evoked EPSCs from thalamic and intracortical sources

Таблиця 1. Нормована інтенсивність, %, усереднених ЗПСС, викликаних активацією таламічних та інракортикальних джерел.

	Thalamus	Layer 2	Layer 3	Layer 4	Layer 5	Layer 6
Auditory						
Layer 4	9.0 ± 5.2	2.5 ± 2.1	29.2 ± 4.6	33.3 ± 2.9	19.1 ± 5.1	6.9 ± 1.0
Layer 6	7.9 ± 6.7	1.3 ± 0.6	4.2 ± 2.5	12.7 ± 3.1	29.2 ± 7.3	44.5 ± 2.1
Somatosensory						
Layer 4	9.4 ± 2.9	2.1 ± 2.1	25.0 ± 6.5	42.4 ± 11.5	13.9 ± 6.4	7.2 ± 4.2
Layer 6	8.1 ± 2.3	1.0 ± 0.8	3.0 ± 1.4	9.2 ± 2.7	31.8 ± 3.1	46.9 ± 7.2
Combined						
Layer 4	9.2 ± 3.5	2.2 ± 1.9	26.5 ± 5.9	39.0 ± 10.0	15.8 ± 6.2	7.2 ± 3.2
Layer 6	8.1 ± 4.0	1.1 ± 0.7	3.4 ± 1.8	10.5 ± 3.2	30.8 ± 4.8	46.0 ± 5.8

Footnote: Means ± s. d. are shown

those to layer 4 (Figs. 5E, 6E) (layer 6 to 4 ratio: A1, 86 ± 24%; S1, 89 ± 19%; combined, 88 ± 21%).

The similar functional topography of the thalamic inputs contrasted with different input patterns from intracortical laminar sources to layers 4 and 6. In general, layer-4 neurons received the bulk of total evoked current from layer 3 (A1, 29.2 ± 4.6%; S1, 25.0 ± 6.5%, combined, 26.5 ± 5.9%) and layer 4 (A1, 33.3 ± 2.9%; S1, 42.4 ± 11.5%; combined, 39.0 ± ± 10.0%) (Figs. 5C, F; 6C, F; Table 1). In comparison, layer 6 received the bulk of evoked current from layer 5 (A1, 29.2 ± 7.3%, S1, 31.8 ± 3.1%; combined, 30.8 ± ± 4.8%) and layer 6 (A1, 44.5 ± 2.1%; S1, 46.9 ± ± 7.2%; combined, 46.0 ± 5.8%) (Figs. 5D, F; 6D, F; Table 1). The proportion of evoked currents from these laminar sources to neurons in layers 4 and 6 was statistically different (*t*-test, $p<0.01$; Table 1). In comparison with the thalamic evoked currents, intracortical sources provided approximately 90% of the total evoked current, while thalamic sources contributed less than 10% (Figs. 5F, 6F, 7; Table 1).

DISCUSSION

Ascending thalamo-cortical axons innervate layers 4 and 6 of the primary auditory and somatosensory cortices [1-4]. Using laser-scanning photostimulation via uncaging of glutamate to map the functional convergence of thalamo-cortical inputs, we found that neurons in layers 4 and 6 in a cortical column receive functional inputs from the same thalamic region. In our experiments, we recorded primarily from young animals whose synaptic properties and connectivity may be undergoing rapid changes [39-41]. Although the relative proportion and spatial distribution of excitatory inputs were similar for all animals in our study, we did not directly assess convergence from intracortical inhibitory sources [42, 43], which may be still developing at this time point [39, 41].

Our results are consistent with previous studies of the functional topography of the thalamo-cortical pathways [9, 44, 45]. In their study, Bureau et al. [44] found that the thalamic inputs from the lemniscal and paralemniscal nuclei (VPm and POm) to the somatosensory cortex were interdigitated, such that POm projected primarily to layer 5a, while VPm projections to layers 4, 5b, and 6 overlapped for pairs in the same column. Here, we found a similar alignment of thalamic projections to layer-4 and layer-6 neurons in the somatosensory barrel cortex [46], which we also observed in the auditory thalamo-cortical projections to layers 4 and 6 of A1. This suggests that a similar topographic principle organizes the TC projections in both systems, and this, perhaps, extends to other modalities, such as the visual system [8].

This pattern of functional convergence revealed by LSPS mapping of thalamo-cortical projections is supported by the pattern of divergence revealed by optical imaging methods [34, 35, 47-57]. Although we observed that electrical stimulation of the thalamus resulted in similar temporal patterns of activation in these layers of the auditory and somatosensory cortices (also similar to observations in previous studies [48, 49, 51-54]), the autofluorescence imaging method that we employed does not enable the fine temporal discrimination available with voltage-

sensitive dyes, which has revealed possible laminar latency differences in the auditory cortex [55]. Our experiments and other previous studies allowed one to observe robust flavoprotein activation in layers 4 and 6 of the auditory and somatosensory cortices following thalamic electrical and photostimulation, but typically with a more prominent activity in layer 6 [35, 47]. Our finding of relatively weaker activity in layer 6 matches more closely that observed by Broicher et al. [55], who used voltage-sensitive dyes and attributed laminar intensity differences in the A1 to the interaction of intracortical circuits. Our findings may result from similar intrinsic mechanisms or methodological ones, such as the intensity of stimulation and, perhaps, less antidromic activation of layer-6 cortico-thalamic neurons. Still, the spatial distribution of activity in layers 4 and 6 observed in this and previous studies suggest that feedforward and feedback projections are likely topographically aligned.

Despite the similar functional topography of the thalamic inputs, the intracortical inputs to layers 4 and 6 differed from each other. We found that layer 4 received predominant inputs from layers 3 and 4, while layer 6 received predominant inputs from layers 5 and 6; this is similar to the distributions observed in prior studies [24, 45, 58-63]. In general, local connectivity within a layer tends to predominate for each layer [60], although area-specific differences in local circuits do exist, such as the respective parallel layer 4- and 5a-projections to layers 2 and 3 in the barrel and septal regions of the S1 [64, 65] and the asymmetric layer-6 projections to layer 3 in the A1 [45]. These functional patterns of connectivity align with the morphological distributions of local circuit axons observed in layers 4 and 6 of the cat A1 [30, 66-71]. As such, the laminar differences in local circuit connectivity provide a morphological basis for the differences in receptive field properties observed between layers 4 and 6 [13-18]. In this respect, while the same basic features of the receptive field are inherited from thalamic sources [72, 73], the subsequent and ongoing recruitment of local intracortical sources likely sculpt responsive refinements, e.g., the observed temporal and modulation preferences in layers 4 and 6 of the A1 [14].

Finally, we found that the thalamo-cortical projections account for approximately 10% of the total evoked current in both layers from the thalamic and intracortical sources. Interestingly, these values are similar in the magnitude to anatomical estimates of the proportion of thalamic and intracortical synapses in layer 4 [22, 23] and the proportion of thalamic neurons converging across layers [20, 74]. This suggests a relative equivalence in the efficacy of the thalamic and intracortical projections, which anatomically contribute nearly half of the total convergent inputs to an area [19-23, 75] and is consistent with the notion of synchronous convergent thalamic synapses that are weak individually [76]. This arrangement may also be necessary for the fewer thalamic inputs to activate the more numerous intracortical projections, which may amplify and process the ascending signals [52, 77-80], resulting in the observed differences in laminar receptive field properties among layers. The thalamo-cortical recruitment of intracortical circuits, both excitatory and inhibitory, may also account for the differences in cortical dynamic responses to transient and sustained activity [81]. Thus, the functional circuitry of the sensory forebrain is comprised of convergent thalamo-cortical pathways that lead to computationally divergent outcomes emerging from concurrent intracortical projections.

The Institutional Animal Care and Use Committee of the Louisiana State University School of Veterinary Medicine approved all experimental procedures.

The authors, Ch. C. Lee and K. Imaizumi, confirm that they have no conflict of interest.

We thank B. Suter and B. Theyel for their assistance with custom analysis software, X. Wu for assistance with confocal microscopy, and P. Venkatadri and C. Burgess for technical assistance. This work was supported by the NIH/NIDCD grant R03 DC 11361, SVM USDA CORP grants LAV3300 and LAV3202, NSF-LA EPSCoR grant PFUND276, and Louisiana Board of Regents RCS grant RD-A-09.

Ч. Лі[1], Л. Імаізумі[1]

ФУНКЦІОНАЛЬНА КОНВЕРГЕНЦІЯ ТАЛАМІЧНИХ ТА ІНТРАКОРТИКАЛЬНИХ ПРОЕКЦІЙ ДО КОРТИКАЛЬНИХ ШАРІВ 4 ТА 6

[1] Луїзіанський університет ветеринарної медицини, Батон Рут (США).

Р е з ю м е

Висхідний потік сенсорної інформації передається з таламуса до шарів 4 та 6 сенсорних кортикальних зон. Цікавим є те, що властивості рецептивних полів у нейронів кортикального шару 6 є відмінними від таких у шарі 4. Чи відображають дані відмінності специфічні природжені патерни таламічних зв'язків або вони зумовлені специфікою локальних кортикальних нейронних мереж? Щоб зробити вибір між такими можливостями, ми використали слайсові препарати *in*

vitro, котрі вміщували таламо-кортикальні шляхи слухової та соматосенсорної систем. Застосовуючи методику петч-клемп у конфігурації «ціла клітина», ми відводили відповіді нейронів шарів 4 та 6, розташованих в одній і тій самій кортикальній колонці. Для отримання карт функціональної топографії таламо-кортикальних та інтракортикальних входів, до кожного із шарів ми використовували методику лазерної скануючої стимуляції, що забезпечувала вивільнення глутамату в таламусі та корі. Окрім того, ми оцінювали функціональну дивергенцію таламо-кортикальних входів за допомогою візуалізації аутофлуоресценції флавопротеїнів. Було виявлено, що таламо-кортикальні входи до шарів 4 та 6 походили від ідентичних таламічних регіонів, тоді як інтракортикальні проекції до одних і тих самих нейронів значно відрізнялися. Наші результати примушують думати, що саме інтракортикальні проекції того або іншого шару, а не таламічні входи в більшій мірі визначають відмінності відповідних рецептивних полів у згаданих шарах.

REFERENCES

1. C. L. Huang and J. A. Winer, "Auditory thalamocortical projections in the cat: laminar and areal patterns of input," *J. Comp. Neurol.*, **427**, 302-331 (2000).
2. P. H. Smith, D. J. Uhlrich, K. A. Manning, and M. I. Banks, "Thalamocortical projections to rat auditory cortex from the ventral and dorsal divisions of the medial geniculate nucleus," *J. Comp. Neurol.*, **520**, 34-51 (2012).
3. P. Landry and M. Deschênes, "Intracortical arborizations and receptive fields of identified ventrobasal thalamocortical afferents to the primary somatic sensory cortex in the cat," *J. Comp. Neurol.*, **199**, 345-372 (1981).
4. A. L. Humphrey, M. Sur, D. J. Ulrich, and S. M. Sherman, "Termination patterns of individual X- and Y-cell axons in the visual cortex of the cat: projections to area 18, to the 17/18 border region, and to both areas 17 and 18," *J. Comp. Neurol.*, **233**, 190-212 (1985).
5. M. Beierlein and B. W. Connors, "Short-term dynamics of thalamocortical and intracortical synapses onto layer 6 neurons in neocortex," *J. Neurophysiol.*, **88**, 1924-1932 (2002).
6. H. J. Rose and R. Metherate, "Auditory thalamocortical transmission is reliable and temporally precise," *J. Neurophysiol.*, **94**, 2019-2030 (2005).
7. K. J. Stratford, K. Tarczy-Hornoch, K. A. Martin, et al., "Excitatory synaptic inputs to spiny stellate cells in cat visual cortex," *Nature*, **382**, 258-261 (1996).
8. J. N. MacLean, V. Fenstermaker, B. O. Watson, and R. Yuste, "A visual thalamocortical slice," *Nat. Methods*, **3**, 129-134 (2006).
9. C. C. Lee and S. M. Sherman, "Synaptic properties of thalamic and intracortical intputs to layer 4 of the first- and higher-order cortical areas in the auditory and somatosensory systems," *J. Neurophysiol.*, **100**, 317-326 (2008).
10. S. M. Sherman and R. W. Guillery, "On the actions that one nerve cell can have on another: distinguishing 'drivers' from 'modulators'," *Proc. Natl. Acad. Sci. USA*, **95**, 7121-7126 (1998).
11. C. C. Lee and S. M. Sherman, "On the classification of pathways in the auditory midbrain, thalamus, and cortex," *Hear. Res.*, **276**, 79-87 (2011).
12. C. C. Lee and S. M. Sherman, "Drivers and modulators in the central auditory pathways," *Front. Neurosci.*, **4**, 79-86 (2010).
13. C. D. Gilbert, "Laminar differences in receptive field properties of cells in cat primary visual cortex," *J. Physiol.*, **268**, 391-421 (1977).
14. C. A. Atencio and C. E. Schreiner, "Laminar diversity of dynamic sound processing in cat primary auditory cortex," *J. Neurophysiol.*, **103**, 192-205 (2010).
15. R. W. Dykes and Y. Lamour, "An electrophysiological study of single somatosensory neurons in rat granular cortex serving the limbs: a laminar analysis," *J. Neurophysiol.*, **70**, 703-724 (1988).
16. L. M. Martinez, Q. Wang, R. C. Reid, et al., "Receptive field structure varies with layer in the primary visual cortex," *Nat. Neurosci.*, **8**, 372-379 (2005).
17. J. C. Brumberg, D. J. Pinto, and D. J. Simons, "Cortical columnar processing in the rat whisker-to-barrel system," *J. Neurophysiol.*, **82**, 1808-1817 (1999).
18. M. N. Wallace and A. R. Palmer, "Laminar differences in the response properties of cells in the primary auditory cortex," *Exp. Brain Res.*, **184**, 179-191 (2008).
19. C. C. Lee and J. A. Winer, "Connections of cat auditory cortex: III. Corticocortical system," *J. Comp. Neurol.*, **507**, 1920-1943 (2008).
20. C. C. Lee and J. A. Winer, "Convergence of thalamic and cortical pathways in cat auditory cortex," *Hear. Res.*, **274**, 85-94 (2011).
21. C. C. Lee and J. A. Winer, "A synthesis of auditory cortical connections: thalamocortical, commissural, and corticocortical systems," in: *The Auditory Cortex*, J. A. Winer and C. E. Schreiner (eds.), Springer, New York (2011), pp. 147-170.
22. T. Binzegger, R. Douglas, and K. Martin, "A quantitative map of the circuit of cat primary visual cortex," *J. Neurosci.*, **24**, 8441-8453 (2004).
23. B. Ahmed, J. C. Anderson, R. J. Douglas, et al., "Polyneuronal innervation of spiny stellate neurons in cat visual cortex," *J. Comp. Neurol.*, **341**, 39-49 (1994).
24. C. C. Lee and S. M. Sherman, "Modulator property of the intrinsic cortical projections from layer 6 to layer 4," *Front. Syst. Neurosci.*, **3**, 3 (2009).
25. C. C. Lee and S. M. Sherman, "Intrinsic modulators of auditory thalamocortical transmission," *Hear. Res.*, **287**, 43-50 (2012).
26. C. C. Lee, Y. W. Lam, and S. M. Sherman, "Intracortical convergence of layer 6 neurons," *NeuroReport*, **23**, 736-740 (2012).
27. S. J. Cruikshank, H. J. Rose, and R. Metherate, "Auditory thalamocortical synaptic transmission *in vitro*," *J. Neurophysiol.*, **87**, 361-384 (2002).
28. A. Agmon and B. W. Connors, "Thalamocortical responses of mouse somatosensory (barrel) cortex *in vitro*," *Neuroscience*, **41**, 365-379 (1991).
29. J. A. Winer and C. C. Lee, "The distributed auditory cortex," *Hear. Res.*, **229**, 3-13 (2007).
30. J. A. Winer and J. J. Prieto, "Layer V in cat primary auditory cortex (AI): cellular architecture and identification of projection neurons," *J. Comp. Neurol.*, **434**, 379-412 (2001).
31. C. C. Lee and S. M. Sherman, "Glutamatergic inhibition in sensory neocortex," *Cerebr. Cortex*, **19**, 2281-2289 (2009).
32. B. A. Suter, T. O'Connor, V. Iyer, et al., "Ephus: multipurpose data acquisition software for neuroscience experiments,"

Front. Neural Circuit., **4**, 100 (2010).
33. C. C. Lee and S. M. Sherman, "Topography and physiology of ascending streams in the auditory tectothalamic pathway," *Proc. Natl. Acad. Sci. USA*, **107**, 372-377 (2010).
34. B. B. Theyel, D. A. Llano, N. P. Issa, et al., "*In vitro* imaging using laser photostimulation with flavoprotein autofluorescence," *Nat. Protoc.*, **6**, 502-508 (2011).
35. B. B. Theyel, C. C. Lee, and S. M. Sherman, "Specific and nonspecific thalamocortical connectivity in the auditory and somatosensory thalamo-cortical slices," *NeuroReport*, **21**, 861-864 (2010).
36. D. A. Llano and S. M. Sherman, "Evidence for non-reciprocal organization of the mouse auditory thalamocortical-corticothalamic projections systems," *J. Comp. Neurol.*, **507**, 1209-1227 (2008).
37. J. A. Winer, J. J. Diehl, and D. T. Larue, "Projections of auditory cortex to the medial geniculate body of the cat," *J. Comp. Neurol.*, **430**, 27-55 (2001).
38. I. Reichova and S. M. Sherman, "Somatosensory corticothalamic projections: distinguishing drivers from modulators," *J. Neurophysiol.*, **92**, 2185-2197 (2004).
39. D. H. Sanes and V. C. Kotak, "Developmental plasticity of auditory cortical inhibitory synapses," *Hear. Res.*, **279**, 140-148 (2011).
40. R. S. Erzurumlu and P. Gaspar, "Development and critical period plasticity of the barrel cortex," *Eur. J. Neurosci.*, **35**, 1540-1553 (2012).
41. A. M. Oswald and A. D. Reyes, "Development of inhibitory timescales in auditory cortex," *Cerebr. Cortex*, **21**, 1351-1361 (2011).
42. Y. Zhou, B. H. Liu, G. K. Wu, et al., "Preceding inhibition silences layer 6 neurons in auditory cortex," *Neuron,* **65**, 706-717 (2010).
43. M. Wehr and A. M. Zador, "Balanced inhibition underlies tuning and sharpens spike timing in auditory cortex," *Nature,* **426**, 442-446 (2003).
44. I. Bureau, F. von Saint Paul, and K. Svoboda, "Interdigitated paralemniscal and lemniscal pathways in the mouse barrel cortex," *PLoS Biol.*, **4**, e382 (2006).
45. H. V. Oviedo, I. Bureau, K. Svoboda, and A. M. Zador, "The functional asymmetry of auditory cortex is reflected in the organization of local cortical circuits," *Nat. Neurosci.*, **13**, 1413-1420 (2010).
46. V. C. Wimmer, R. M. Bruno, C. P. de Kock, et al., "Dimensions of a projection column and architecture of VPM and POm axons in rat vibrissal cortex," *Cerebr. Cortex*, **20**, 2265-2276 (2010).
47. D. A. Llano, B. B. Theyel, A. K. Mallik, et al., "Rapid and sensitive mapping of long-range connections in vitro using flavoprotein autofluorescence imaging combined with laser photostimulation," *J. Neurophysiol.*, **101**, 3325-3340 (2009).
48. S. Higashi, M. C. Crair, T. Kurotani, et al., "Altered spatial patterns of functional thalamocortical connections in the barrel cortex after neonatal infraorbital nerve cut revealed by optical recording," *Neuroscience*, **91**, 439-452 (1999).
49. N. Laaris, G. C. Carlson, and A. Keller, "Thalamic-evoked synaptic interactions in barrel cortex revealed by optical imaging," *J. Neurosci.*, **20**, 1529-1537 (2000).
50. T. A. Hackett, T. R. Barkat, B. M. O'Brien, et al., "Linking topography to tonotopy in the mouse auditory thalamocortical circuit," *J. Neurosci.*, **31**, 2983-2995 (2011).
51. R. R. Llinas, E. Leznik, and F. J. Urbano, "Temporal binding via cortical coincidence detection of specific and nonspecific thalamocortical inputs: a voltage-dependent dye-imaging study in mouse brain slices," *Proc. Natl. Acad. Sci. USA*, **99**, 449-454 (2002).
52. M. Beierlein, C. P. Fall, J. Rinzel, and R. Yuste, "Thalamocortical bursts trigger recurrent activity in neocortical networks: layer 4 as a frequency-dependent gate," *J. Neurosci.*, **22**, 9885-9894 (2002).
53. M. Kubota, S. Sugimoto, J. Horikawa, et al., "Optical imaging of dynamic horizontal spread of excitation in rat auditory cortex slices," *Neuosci. Lett.*, **237**, 77-80 (1997).
54. M. Kubota, M. Nasu, and I. Taniguchi, "Layer-specific horizontal propagation of excitation in the auditory cortex," *NeuroReport*, **10**, 2865–2867 (1999).
55. T. Broicher, H. J. Bidmon, B. Kamuf, et al., "Thalamic afferent activation of supragranular layers in auditory cortex *in vitro*: a voltage sensitive dye study," *Neuroscience*, **165**, 371-385 (2010).
56. S. Kaur, H. J. Rose, R. Lazar, et al., "Spectral integration in primary auditory cortex: laminar processing of afferent input, *in vivo* and *in vitro*," *Neuroscience*, **134**, 1033-1045 (2005).
57. D. Contreras and R. Llinas, "Voltage-sensitive dye imaging of neocortical spatiotemporal dynamics to afferent activation frequency," *J. Neurosci.*, **21**, 9403-9413 (2001).
58. D. L. Barbour and E. M. Callaway, "Excitatory local connections of superficial neurons in rat auditory cortex," *J. Neurosci.*, **28**, 11174-11185 (2008).
59. D. A. Llano and S. M. Sherman, "Differences in intrinsic properties and local network connectivity of identified layer 5 and layer 6 adult mouse auditory corticothalamic neurons support a dual corticothalamic projection hypothesis," *Cerebr. Cortex*, **19**, 2810-2826 (2009).
60. B. M. Hooks, S. A. Hires, Y. X. Zhang, et al., "Laminar analysis of excitatory local circuits in vibrissal motor and sensory cortical areas," *PLoS Biol.*, **9**, e1000572 (2011).
61. A. Zarrinpar and E. M. Callaway, "Local connections to specific types of layer 6 neurons in the rat visual cortex," *J. Neurophysiol.*, **95**, 1751-1761 (2006).
62. Y. Yoshimura, J. L. Dantzker, and E. M. Callaway, "Excitatory cortical neurons form fine-scale functional networks," *Nature*, **433**, 868-873 (2005).
63. F. Briggs and E. M. Callaway, "Layer-specific input to distinct cell types in layer 6 of monkey primary visual cortex," *J. Neurosci.*, **15**, 3600-3608 (2001).
64. G. M. Shepherd, A. Stepanyants, I. Bureau, et al., "Geometric and functional organization of cortical circuits," *Nat. Neurosci.*, **8**, 782-790 (2005).
65. G. M. Shepherd, T. A. Pologruto, and K. Svoboda, "Circuit analysis of experience-dependent plasticity in the developing rat barrel cortex," *Neuron*, **38**, 277-289 (2003).
66. H. Ojima, C. N. Honda, and E. G. Jones, "Patterns of axon collateralization of identified supragranular pyramidal neurons in the cat auditory cortex," *Cerebr. Cortex*, **1**, 80-94 (1991).
67. H. Ojima, C. N. Honda, and E. G. Jones, "Characteristics of intracellularly injected infragranular pyramidal neurons in cat primary auditory cortex," *Cerebr. Cortex*, **2**, 197-216 (1992).
68. J. A. Winer, "Anatomy of layer IV in cat primary auditory cortex (AI)," *J. Comp. Neurol.*, **224**, 535-567 (1984).
69. J. A. Winer, "The non-pyramidal neurons in layer III of cat primary auditory cortex (AI)," *J. Comp. Neurol.*, **229**, 512-530 (1984).
70. J. A. Winer, "The pyramidal cells in layer III of cat primary

auditory cortex," *J. Comp. Neurol.*, **229**, 476-496 (1984).
71. J. J. Prieto and J. A. Winer, "Layer VI in cat primary auditory cortex: Golgi study and sublaminar origins of projection neurons," *J. Comp. Neurol.*, **404**, 332-358 (1999).
72. J. A. Winer, L. M. Miller, C. C. Lee, and C. E. Schreiner, "Auditory thalamo-cortical transformation: structure and function," *Trends Neurosci*, **28**, 255-263 (2005).
73. L. M. Miller, M. A. Escabí, H. L. Read, and C. E. Schreiner, "Functional convergence of response properties in the auditory thalamo-cortical system," *Neuron*, **32**, 151-160 (2001).
74. C. C. Lee and J. A. Winer, "Connections of cat auditory cortex: I. Thalamo-cortical system," *J. Comp. Neurol.*, **507**, 1879-1900 (2008).
75. J. W. Scannell, C. Blakemore, and M. P. Young, "Analysis of connectivity in the cat cerebral cortex," *J. Neurosci.*, **15**, 1463-1483 (1995).
76. R. M. Bruno and B. Sakmann, "Cortex is driven by weak but synchronously active thalamo-cortical synapses," *Science*, **312**, 1622-1627 (2006).
77. R. J. Douglas, C. Koch, M. Mahowald, et al., "Recurrent excitation in neocortical circuits," *Science*, **269**, 981-985 (1995).
78. R. Ben-Yishai, R. L. Bar-Or, and H. Sompolinsky, "Theory of orientation tuning in visual cortex," *Proc. Natl. Acad. Sci. USA*, **92**, 3844-3848 (1995).
79. B. H. Liu, G. K. Wu, R. Arbuckle, et al., "Defining cortical frequency tuning with recurrent excitatory circuitry," *Nat. Neurosci.*, **10**, 1594-1600 (2007).
80. J. N. MacLean, B. O. Watson, G. B. Aaron, and R. Yuste, "Internal dynamics determine the cortical response to thalamic stimulation," *Neuron*, **8**, 811-823 (2005).
81. C. R. Stoelzel, Y. Bereshpolova, A. G. Gusev, and H. A. Swadlow, "The impact of an LGNd impulse on the awake visual cortex: synaptic dynamics and the sustained/transient distinction," *J. Neurosci.*, **28**, 5018-5028 (2008).